MICROSTRUCTURAL AND MECHANICAL CHARACTERISATION OF AL BACK CONTACT LAYERS AND ITS APPLICATION TO THERMOMECHANICAL MULITSCALE MODELLING OF SOLAR CELLS

V.A. Popovich¹, T. van Amstel², I. J. Bennett², M. Janssen¹, I.M.Richardson¹

1. Delft University of Technology, Department of Materials Science & Engineering, Delft, The Netherlands,

Phone: +31 (0) 15 27 895 68, email: v.popovich@tudelft.nl

2. Energy Research Centre of the Netherlands, Solar Energy, PV Module Technology, Petten, The Netherlands

ABSTRACT

The overall demand to reduce the solar energy costs gives a continuous drive to reduce the thickness of silicon wafers. Handling and bowing problems associated with thinner wafers become more and more important, as it can lead to cells cracking and high yield losses. This paper discusses the microstructure and mechanical properties of the aluminium on the rear side of a solar cell. It will be shown that the aluminium back contact has a complex compositelike microstructure, consisting of five main components: 1) back surface field layer 2) eutectic layer 3) spherical (3 - 5 µm) hypereutectic Al-Si particles, surrounded by a thin aluminum oxide layer (200 nm); 4) a bismuth-silicate glass matrix; 5) pores (15 vol.%). The Young's modulus of the Al-Si particles is estimated by nanoindentation. These results are used as input parameters for an improved thermomechanical multiscale model of a silicon solar cell.

Keywords: Al back contact, microstructure, Young's modulus, Multiscale model

INTRODUCTION

The most critical processing step during the manufacture of screen-printed solar cells is the firing process. Residual stresses are formed within the cell due to thermal coefficients mismatch and different mechanical behaviour of the materials used in the metallic contacts. The wafer bows and forms a convex body upon cooling, which may result in the actual fracture of the cells [1].

As the thickness of silicon wafers is reduced, cell bowing becomes a major problem during different processing steps. It is possible to decrease bowing by reducing the amount of aluminium paste or by changing the paste chemistry and firing conditions. However, there is a limit below which screen-printed aluminium paste will lead to a non-uniform back surface field layer, influencing the electrical properties of the cell [2-4]. Nowadays it is very important to find a compromise between electrical properties, strength and the cost of the solar cell. To this aim it is necessary to have a better understanding of microstructure, stress development and mechanical properties of the cell.

The aim of this paper is to investigate microstructure and mechanical properties of the aluminium at the rear side of the solar cell and apply these results in a novel thermomechanical multiscale model. On the basis of this knowledge it should be possible to determine mechanical limits of the solar cell with the aim of reducing yield losses during cell and module manufacture.

EXPERIMENTAL

A JEOL JSM 6500F scanning electron microscope (SEM) with energy-dispersive spectroscopy (EDS) was used for microstructural analysis of cleaved samples of a conventional H-pattern solar cell. In order to identify the Al-Si reaction layer samples were polished and etched in a solution of HF-HNO₃-CH₃COOH (1:3:6) for 20 seconds. Metallic polishing holders were used to prevent any influence of the embedding resin to microstructure analysis. Apart from EDS, an accurate compositional determination was performed by electron probe micro analyses (EPMA).

Phase identification of the as-dried and sintered Al pastes was conducted by X-ray Diffraction using a D8-discover diffractometer (Cu K_{α} radiation) equipped with an Euler cradle. A multiphase structure refinement was carried out by means of a full profile Rietveld method including refinement of the lattice parameters, atomic positions, scale factor, zero shift, background and Bragg-peak profile parameters. Starting models for the calculation procedure were taken from the inorganic crystal structure database (ICSD).

The high-resolution computed tomography ("Nanotom" system) equipped with a high-power nanofocused tube (180 kV/15 W) was used for a microstructural characterization of the AI bulk layer and a concentration profile determination of glass phases in the as-fired AI paste. This technique provides a three-dimensional spatial image of an object, showing different materials in different colors according to to their density. Computed tomography 3D images were generated by a rotation of the sample with a step of 0.5° for 360° around a rotational axis, while taking a series of 2D pictures. Afterwards these images were combined to create a 3D volumetric representation of the structure using a complex reconstruction algorithm.

Mercury intrusion porosimetry (MIP) was performed on small (30x10 mm) samples to determine the pore volume, porosity and the pore size distribution in the AI rear face layer. This technique is based on the principle that mercury is a non-wetting liquid and requires a force to penetrate voids. The experiments were performed on a CE instrument Pascal 140 (low pressure) and Pascal 440 (high pressures) in a pressure range from 0.01 kPa to 400 MPa

Elastic properties of solar cell cross section layers were characterized by a nanoindentation technique using MT5 Nanoindenter G200 instrument, capable of continuous stiffness measurements. Before experiments, samples were embedded into the Epofix resin for a better support during indentation. The tester was equipped with a three-side pyramid (Berkovich) diamond indenter with a 50 nm in radius. Nanoindentation results were averaged over 30 indentations, made for every sample. Young's modulus was evaluated according to the Oliver and Pharr approach [5].

RESULTS AND DISCUSSION

Fig. 1(a) shows polished and etched SEM cross section of a typical screen printed silicon solar cell microstructure consisting of 5 distinct layers: silver, silicon, back surface field (BSF), eutectic and fired Al paste. The bulk aluminum layer was found to have a complex porous microstructure. A closer look into the bulk Al layer (Fig. 1 (b)) reveals the presence of spherical particles, surrounded by a distinct oxide layer. The thickness of this oxide layer is

about 150-200 nm, which is in good agreement with TGA experiments (not presented here) showing a (partial) oxidation of the aluminum in the sample by a mass increase around 600 °C. Electron probe micro analysis confirmed an increase of oxygen concentration around the particle edges.

This oxide layer creates a shell around the particle, which holds the particles in place, and thus creates a stable microstructure of the paste. It is expected that a particle-to-particle contact is made by the oxide layer, which might reduce the particle bonding force and affect the mechanical properties of the layer. EDS results showed that these spherical particles have nearly eutectic Al-Si composition, surrounded by a complex matrix of Al, Si and O (Fig. 2). X-ray elements mapping also showed the presence of Bi and Ca, which is a residue from the initial Al paste composition.

An XRD analysis was performed on the back surface of the cell in order to indentify phases present in the Al layer. Measurements were done for both mechanically removed Al layer and as processed layer on top of the Si wafer. Fig. 3 represents the X-ray spectrum of the Al paste, mechanically removed after firing. Besides the expected Al and Si, three extra phases were detected, namely $\gamma\text{-Al}_2O_3$, CaMgSiO_4, and bismuth silicon oxide. The latter two are a residue of the initial glass frit present in the Al paste to obtain better sintering properties of the contact layer. The presence of the $\gamma\text{-Al}_2O_3$ is in good agreement with literature results, showing a formation of amorphous alumina between 300 to 550 °C and its further transformation into $\gamma\text{-Al}_2O_3$ at about 550 °C [6].

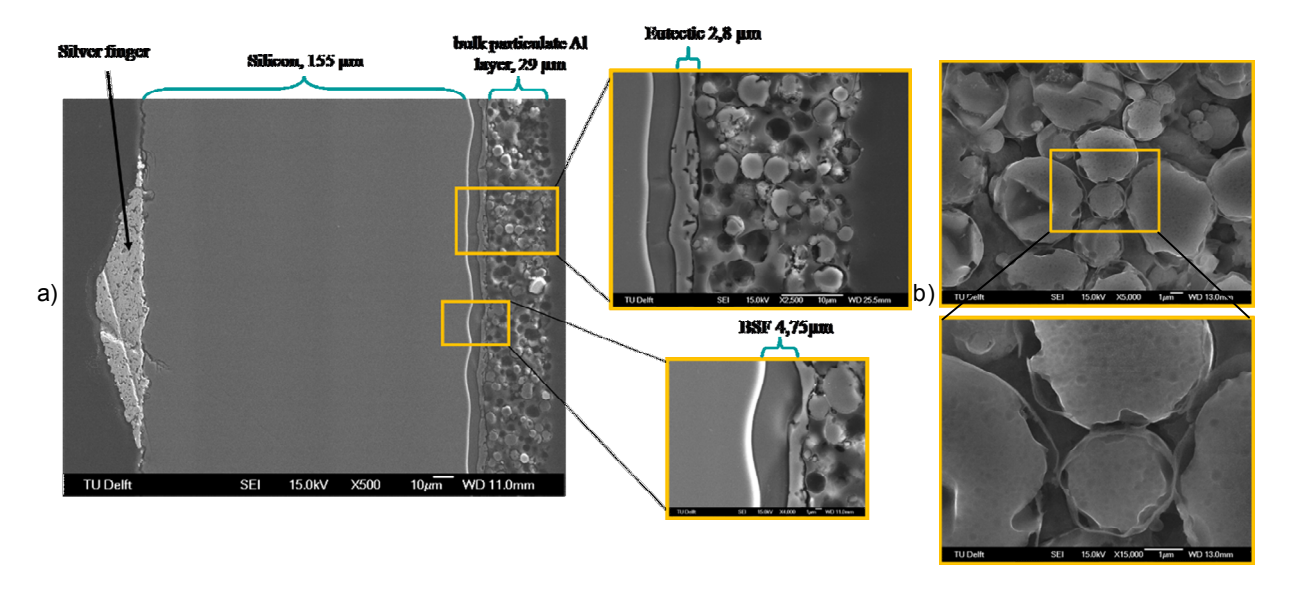


Fig. 1. (a) SEM micrograph of cross section of a conventional silicon solar cell (155×155 mm², 160 μm), representing 5 distinct layers; b) Microstructure of bulk Al layer with Al-Si spherical particles, surrounded by a thin film of alumina.

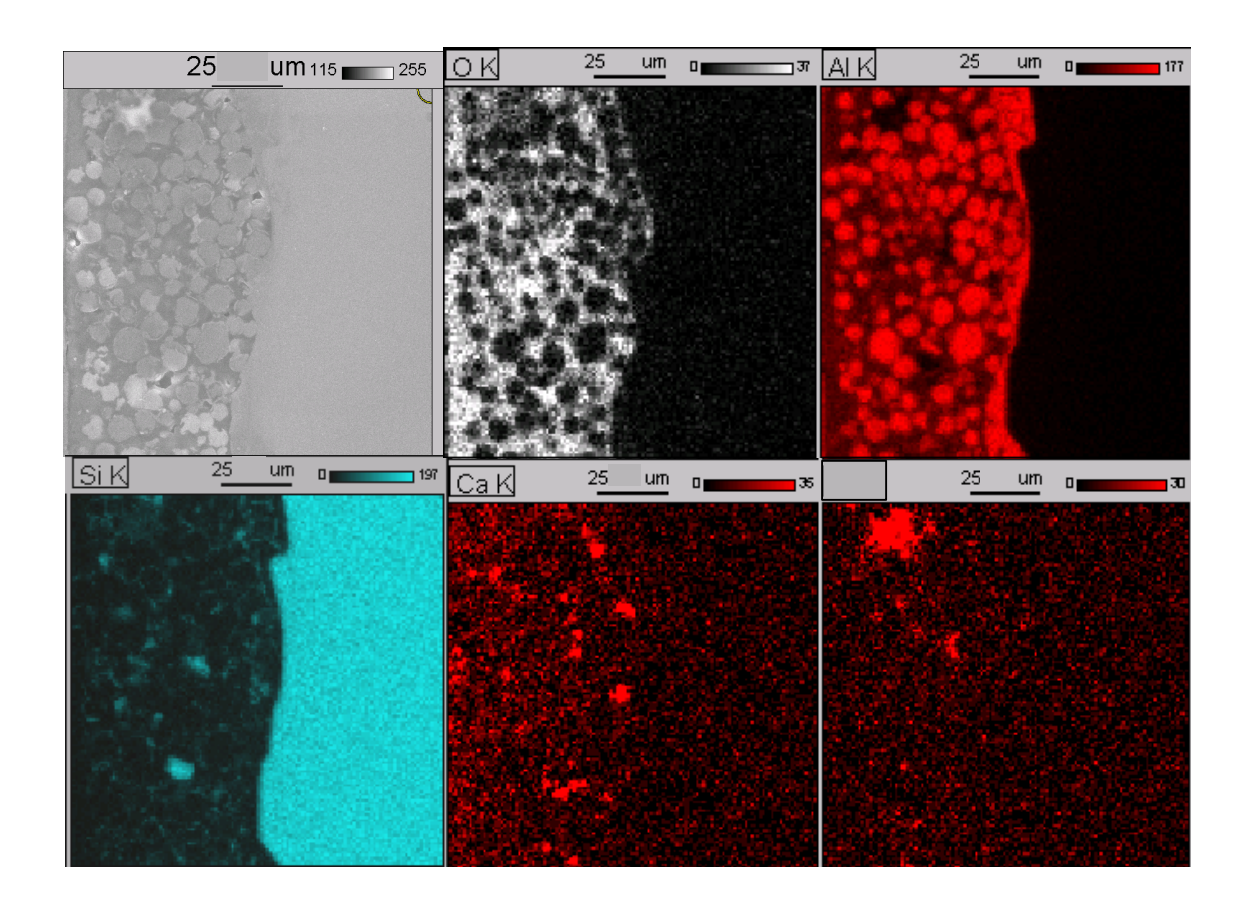


Fig. 2. X-ray element mapping of the Al-Si cross section, indicating the location of selected elements.

In order to evaluate the ratio between Al and Si in the Al back surface layer a full profile Rietveld Refinement was performed, employing FullProf software. As a starting model for the refinement bulk Al and Si structures were used; glass phases were not included in the refinement. The refinement provided a good agreement between observed and calculated profiles. The estimated weight ratio between Al and Si, e.g. 83%:17% is found in a good agreement with EDS/EPMA results.

A computer tomography analysis was carried out to obtain the percentage of bismuth silicate glass. Fig. 4 shows a representative 2D X-ray image of the Al layer. Yellow parts correspond to a higher atomic number material (bismuth, Z=83), which absorbs more X-rays, and grey parts to lower atomic number materials, such as aluminum (Z=13) and silicon (Z=14). Based on the digitalized image,

the concentration of the bismuth glass was estimated to be $2.8 \div 2.9\%$ vol.%.

The overall open porosity of the Al layer, estimated by mercury intrusion porosimetry, was found to be around 15%. Results showed that at a relatively low pressure (0.06 MPa) a filling of large pores (around 50 microns) occurs. An increase in pressure (0.5-2 MPa) revealed the filling of the remaining small pores, which are about 2 microns in size.

Fig. 5 shows a representative nanoindentation load-displacement curve and SEM micrograph of the nanoindented Al-Si particle. The Young's modulus of the bulk layer particles was found to be approximately 72 GPa at 1.5 mN, which agrees well with literature results for eutectic Al-Si alloys.

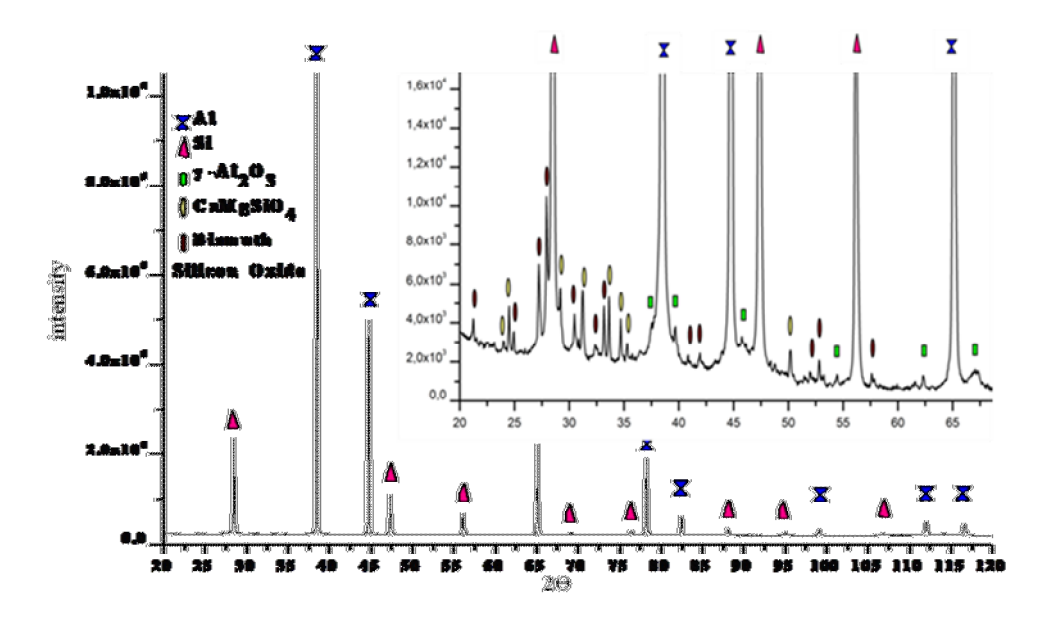


Fig. 3. XRD spectrum of the mechanically removed AI paste after firing. Inset shows an enlarged fragment of the XRD pattern from 2θ =20° to 60°.

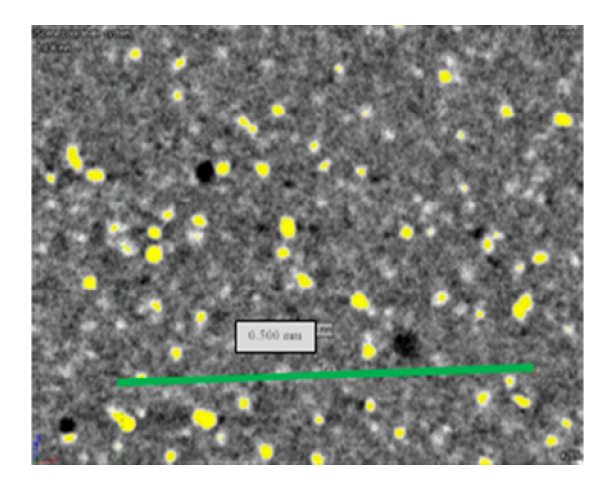


Fig. 4. X-ray image of the Al layer, showing the differences in photographic density between different parts (yellow part: bismuth, black: porosity, grey: Al and Si).

Based on these results, a model was made describing the cross section of the rear face of the silicon solar cell with corresponding microstructure features (Fig. 6). The Al layer is represented as a complex composite-like material, consisting of three main components: 1) spherical (3 - 5 μ m) hypereutectic Al-Si particles, surrounded by a thin aluminum oxide layer (200 nm); 2) a bismuth-silicate glass matrix (2,8 vol.%); 3) pores (15 vol.%).

The results of microstructure and nanoindentation analyses were used in a thermomechanical multiscale model of a solar cell. The model integrates the thermomechanical behaviour of the layers at the rear of the cell, allowing bowing of the whole cell to be predicted. In Fig. 7 an example is given where cell bowing is predicted and related to features at the microscopic level.

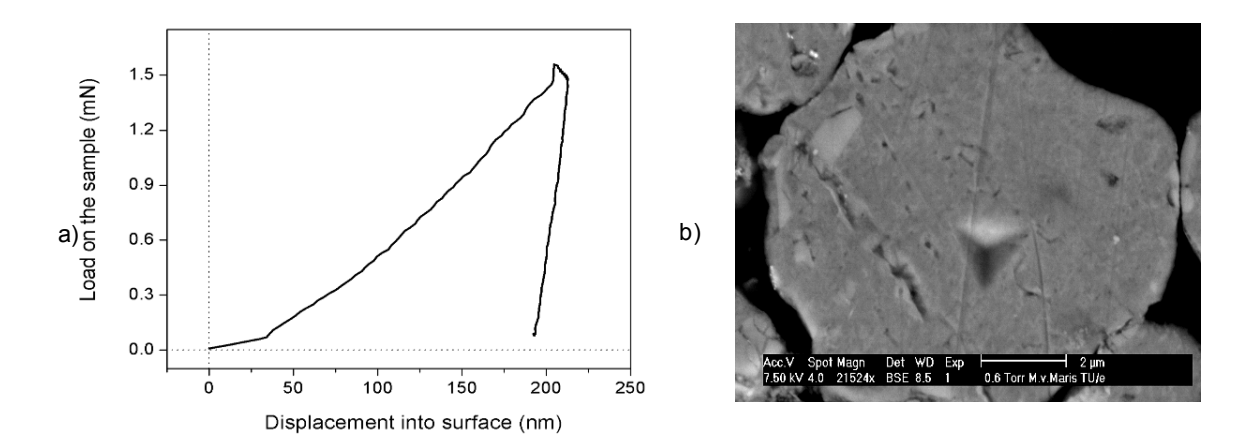


Figure 5. a) Load-displacement curve and b) SEM micrograph of representative nanoindented Al-Si particle.

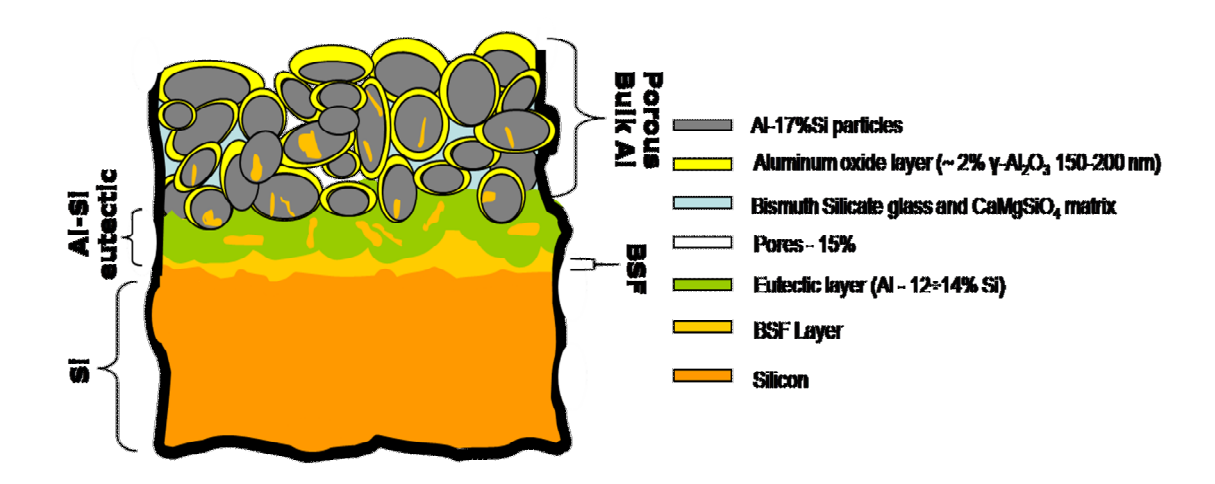


Fig. 6. Model of the rear face of a silicon solar cell with corresponding microstructure features.

These features include morphology, inclusion size and aspect ratio distribution and mechanical properties of inclusions in the aluminium layer. After experimental verification, the model can be used to predict the state of the aluminium microstructure based on measurements of cell bowing.

The multiscale model uses both mean field and finite element homogenization to predict the mechanical response of the porous bulk aluminum Results of this thermomechanical multiscale model will be presented in a follow-up article [7].

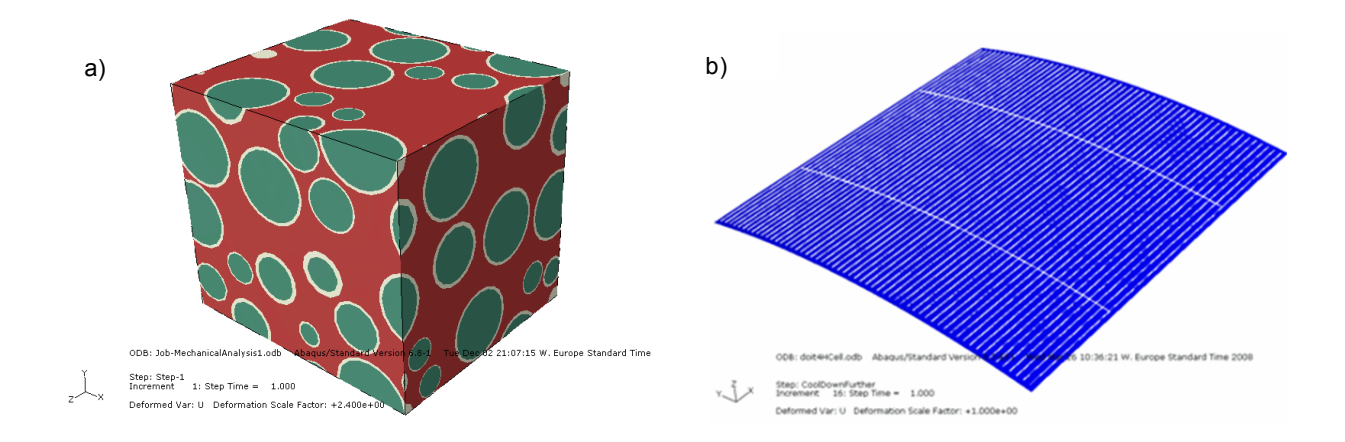


Fig. 7. a) A finite element model of the microstructure of the Al layer. This finite element model is used to fit the homogenization methods, which link the microstructure information with the macroscopic stiffness matrix; b) Predicted cell bowing after firing.

CONCLUSIONS

In this work the microstructure and mechanical properties of the aluminum on the rear face of a solar cell were investigated. It was shown that the AI layer has a complex composite-like microstructure, consisting of three main components: 1) spherical (3 - 5 $\mu m)$ hypereutectic AI-Si particles, surrounded by a thin aluminum oxide layer (150-200 nm); 2) a bismuth-silicate glass matrix (2,8%) 3) pores (15%). The Young's modulus of the AI-Si particles, estimated by nanoindentation, was found to be 72 GPa. These results were used as input parameters for an improved thermomechanical multiscale model of a silicon solar cell, which incorporates the behavior of the various layers.

REFERENCES

[1] T van Amstel, , V.A. Popovich, P. C. de Jong & I. G. Romijn,. Modeling mechanical aspects of the aspire cell. In s.n. (Ed.), Proceedings of the 23rd European Photovoltaic Solar Energy Conference, Valencia, Spain, September 1-5, 2008

[2] F. Huster, "Investigation of the Alloying Process of Screen Printing Aluminum Pastes for the BSF Formation

- on Silicon Solar Cells", 20th European Photovoltaic Solar Energy Conference, Barcelona 2005
- [3] F. Huster, "Aluminum-back surface field: bow investigation and elimination", 20th European Photovoltaic Solar Energy Conference and Exhibition, pp. 635–638, Barcelona, 2005
- [4] S. Kim et al., Aluminum paste (Lead-Free/Low Bow) for thin wafers, IEEE 31st Photovoltaic Specialists Conference and Exhibition, Jan. 3-7, Orlando, Florida, USA, 2004
- [5] W. C. Oliver and G. M. Pharr, "An Improved Technique for Determining Hardness and Elastic Modulus Using Load and Displacement Sensing Indentation Experiments," J. Mater. Res., Vol. 7, No. 6, pp. 1564-1583, 1992.
- [6] M. Trunov et. al., "Effect of Polymorphic phase transformations in Al_2O_3 film on oxidation kinetics of aluminum powders", Comb. and Flame 140, pp.310-318, 2006
- [7] T van Amstel, , V.A. Popovich, P. C. de Jong, I.J. Bennett, (2008) A Multiscale Model of the Aluminium Layer at the Rear Side of a Solar Cell, Proceedings of the 23rd European Photovoltaic Solar Energy Conference, Hamburg, Germany, 2009 (accepted)